

Role of Orbital Degeneracy in the Single Molecule Magnet Behavior of a Mononuclear High-Spin Fe(II) Complex

A. V. Palii,^{*,†} J. M. Clemente-Juan,^{*,‡,§} E. Coronado,[‡] S. I. Klokishner,[†] S. M. Ostrovsky,[†] and O.S. Reu[†]

[†]Institute of Applied Physics, Academy of Sciences of Moldova, Academy Str. 5, MD 2028 Kishinev, Moldova,

[‡]Instituto de Ciencia Molecular, and [§]Fundació General de la Universitat de València (FGUV),
Universidad de Valencia, Polígono de la Coma, s/n 46980 Paterna, Spain

Received June 4, 2010

To explain the single-molecule magnet behavior of the mononuclear complex $[(\text{tpaMes})\text{Fe}]^+$ we have developed a model that takes into account the trigonal ligand field splitting of the atomic ^5D term of the Fe(II) ion, and the spin–orbital splitting and mixing of the ligand field terms. The ground ligand field term is shown to be the orbital doublet ^5E possessing an unquenched orbital angular momentum. We demonstrate that the splitting of this term cannot be described by the conventional zero-field splitting Hamiltonian proving thus the irrelevance of the spin-Hamiltonian formalism in the present case. The first-order orbital angular momentum is shown to lead to the strong magnetic anisotropy with the trigonal axis being the easy axis of the magnetization.

Introduction

The magnetic behavior of single-molecule magnets (SMMs)^{1,2} is characterized by the presence of slow relaxation of magnetization at low temperatures. Such behavior was first discovered in the family of clusters of general formula $[\text{Mn}_{12}\text{O}_{12}(\text{O}_2\text{CR})_{16}(\text{H}_2\text{O})_4]$ known as Mn_{12}ac . Since this discovery, many other SMMs have been synthesized and characterized.

One of the most important characteristics of SMMs is the blocking temperature, which is closely related to the magnitude of the spin reorientation barrier. In spite of the exhausting attempts to increase the blocking temperatures, for existing SMMs they do not exceed a few kelvin, which are too low for application of these systems as data-storage units. This situation looks like as if some natural limit in this route has already been achieved. The origin of this limitation has been recently elucidated by O. Waldmann³ by analyzing the expression for the magnetization reversal barrier for spin-clusters. In these systems the ground states of all constituent metal ions are only characterized by spin, whereas the orbital angular momenta are quenched. For an integer ground state spin S the barrier is defined as $\Delta_b = |D_S|S^2$, where $D_S < 0$ is the axial molecular zero-field splitting (ZFS) parameter for this S -state. The expression for Δ_b shows that the barrier can be increased either by the increase of the anisotropy parameter $|D_S|$ or by the increase of S . The possibility to increase $|D_S|$ is strongly limited because the

ZFS in spin-clusters represents a second-order effect with respect to the spin–orbit coupling⁴ and hence the ZFS is usually weak. The increase of S appeared as a more promising way of design of SMMs with high blocking temperatures because of its expected quadratic influence on Δ_b . It has been, however, demonstrated³ that the parameter D_S is proportional to S^{-2} and hence the barrier Δ_b does not increase as S^2 but as S^0 with the increase of S . This probably explains the fact that all attempts to increase S by the synthesis of big spin-clusters with high values of the ground state spin have not yet produced better SMMs.

The above analysis shows that the conventional design approaches seem to run out of steam and new concepts in the field are required. In this connection the most promising new route is to go beyond the spin-clusters and to exploit the first-order orbital magnetism that is inherently related to the orbitally degenerate metal ions with unquenched orbital angular momenta. The recent studies of SMMs comprising such ions revealed that the spin–orbital splitting in this case appears in the first order of perturbation theory and gives rise to the magnetic anisotropy that is in general much stronger than the second-order anisotropy originating from the ZFS spin-Hamiltonian.^{5–9}

(4) Kahn, O. *Molecular Magnetism*; VCH: New York, 1993.

(5) Palii, A. V.; Ostrovsky, S. M.; Klokishner, S. I.; Tsukerblat, B. S.; Berlinguette, C. P.; Dunbar, K. R.; Galán-Mascarós, J. R. *J. Am. Chem. Soc.* **2004**, *126*, 16860.

(6) Tsukerblat, B. S.; Palii, A. V.; Ostrovsky, S. M.; Kunitsky, S. V.; Klokishner, S. I.; Dunbar, K. R. *J. Chem. Theory Comput.* **2005**, *1*, 668–673.

(7) Palii, A. V.; Ostrovsky, S. M.; Klokishner, S. I.; Tsukerblat, B. S.; Dunbar, K. R. *Chem. Phys. Chem.* **2006**, *7*, 871.

(8) Palii, A. V.; Ostrovsky, S. M.; Klokishner, S. I.; Tsukerblat, B. S.; Schelter, E. J.; Prosvirin, A. V.; Dunbar, K. R. *Inorg. Chim. Acta* **2007**, *360*, 3915.

(9) Palii, A. V. *Phys. Lett. A* **2007**, *365*, 121.

*To whom correspondence should be addressed. E-mail: juan.m.clemente@uv.es (J.M.C.-J.), andrew.palii@uv.es (A.V.P.).

(1) Gatteschi, D.; Sessoli, R.; Villain, J. *Molecular Nanomagnets*; Oxford University Press: Oxford, 2006.

(2) Gatteschi, D.; Sessoli, R. *Angew. Chem., Int. Ed.* **2003**, *42*, 268.

(3) Waldmann, O. *Inorg. Chem.* **2007**, *46*, 10035.

This observation explains the fact that pronounced alternating current (ac) susceptibility signals have been detected in many clusters comprising 3d, 4d, 5d, and 4f metal ions with unquenched orbital angular momenta.^{10–18} Moreover, as distinguished from the conventional SMMs based on polynuclear exchange-coupled clusters, the use of the ions with unquenched orbital angular momenta have recently led to the discovery of SMMs based on a single f-metal ion.^{19–25}

Recently the first example of a SMM based on a mononuclear transition metal complex has been reported by Long with co-workers.²⁶ This system represents the complex $[(\text{tpaMes})\text{Fe}]^-$ formed by a high-spin Fe(II) ion in a trigonal pyramidal environment. Although this complex does not exhibit a slow relaxation at zero applied direct current (dc) field because of the fast quantum tunneling arising from a distortion of the trigonal site, the application of the dc field gives rise to a set of frequency-dependent peaks in the plots of χ_M'' versus ν with varying temperature. To explain these magnetic properties the spin-Hamiltonian with a very large negative D value was used.²⁶ However, this strong magnetic anisotropy has to be assigned to the fact that the Fe(II) ion is orbitally degenerate and possesses a first-order orbital angular momentum. Consequently, in this article we propose a more realistic approach within which we go beyond the spin model to provide an adequate explanation of the observed magnetic behavior of the $[(\text{tpaMes})\text{Fe}]^-$ complex. In this consideration we explicitly take into account the trigonal ligand field (LF) induced by the nearest nitrogen surrounding of the Fe(II) ion and the spin-orbit (SO) splitting of the LF terms. The role of the covalence effects is discussed as well.

Model

The structure of the trigonal pyramidal complex $[(\text{tpaMes})\text{Fe}]^-$ is shown in Figure 1a.^{26,27} The first coordination sphere

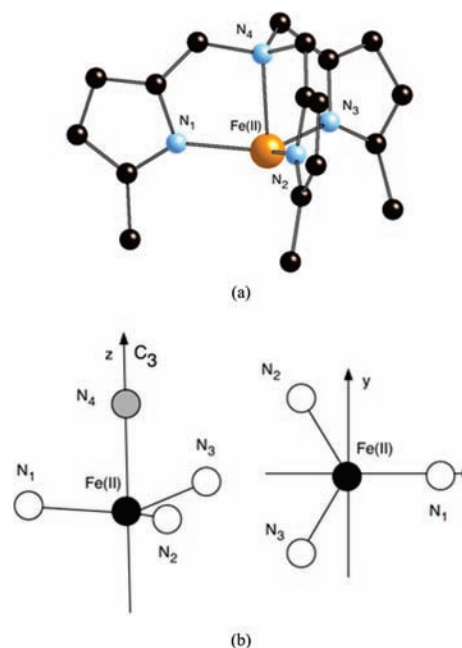


Figure 1. (a) Fragment of the structure of the trigonal pyramidal complex $[(\text{tpaMes})\text{Fe}]^-$ and the structure of the nitrogen atoms of the first coordination sphere. Orange, blue, and gray spheres represent Fe, N, and C atoms, respectively.^{26,27} (b) Structure of the idealized trigonal complex of C_{3v} symmetry (only the atoms of the nearest coordination sphere are shown) together with the Cartesian frame.

Table 1. Spherical Coordinates of the Nitrogen Ligands in the Complex $[(\text{tpaMes})\text{Fe}]^-$ for the Real (Left)²⁷ and the Idealized Trigonal (Right) Geometries

| ligands | spherical coordinates | | | | | |
|----------------|-----------------------|-----------|----------------------|-----------|-----------------------|-----------|
| | $R(\text{\AA})$ | | $\theta(\text{deg})$ | | $\varphi(\text{deg})$ | |
| | real | idealized | real | idealized | real | idealized |
| N ₁ | 2.008 | 2.025 | 82.45 | 82.56 | 0 | 0 |
| N ₂ | 2.04 | 2.025 | 82.01 | 82.56 | 119 | 120 |
| N ₃ | 2.024 | 2.025 | 83.21 | 82.56 | 243.1 | 240 |
| N ₄ | 2.172 | 2.172 | 0 | 0 | 0 | 0 |

of the Fe(II) ion slightly deviates from the C_{3v} symmetry, and to simplify the subsequent analysis we will focus on the idealized trigonal complex of C_{3v} symmetry shown in Figure 1b together with the chosen Cartesian frame. In the LF analysis we will use the spherical coordinates of the nitrogen ligands in the idealized trigonal complex. These coordinates are given in Table 1 along with those for the real complex.

The evaluation of the LF parameters requires the knowledge of the values of the charges for each ligand of the first coordination sphere. It is to be noted that the nature of the nitrogen atom N₄ is quite different from that for atoms N₁, N₂, and N₃, and this determines the difference in their charges. Thus the apical nitrogen atom N₄ is of amino type and hence it is of a non-ionic nature. As a result, this atom is expected to be uncharged ($Z_4 = 0$). On the contrary the three ligands in the plane (N₁, N₂, and N₃) are of pyrrolate type, and a negative charge $Z_1 = Z_2 = Z_3 = Z = 1$ can be associated to each of these atoms. In spite of the fact that the apical ligand N₄ is uncharged, it is expected to play a crucial role in the determination of the LF parameters because the covalence effect for the Fe(II)–N(4) bond is expected to be quite strong. This effect arises from the strong overlap between the d_{z^2} orbital of the Fe(II) ion and the p_z orbital of the N(4) ligand (Figure 2).

- (10) Sokol, J. J.; Hee, A. G.; Long, J. R. *J. Am. Chem. Soc.* **2002**, *124*, 7656.
 (11) Berlinguette, C. P.; Vaughn, D.; Cañada-Vilalta, C.; Galán-Mascarós, J.-R.; Dunbar, K. R. *Angew. Chem., Int. Ed.* **2003**, *42*, 1523.
 (12) Schelter, E. J.; Prosvirin, A. V.; Reiff, W. M.; Dunbar, K. R. *Angew. Chem., Int. Ed.* **2004**, *43*, 4912.
 (13) Tang, J.; Hewitt, I.; Madhu, N. T.; Chastanet, G.; Wernsdorfer, W.; Anson, C. E.; Benelli, C.; Sessoli, R.; Powell, A. K. *Angew. Chem., Int. Ed.* **2006**, *45*, 1729.
 (14) Luzon, J.; Bernot, K.; Hewitt, J. J.; Anson, C. E.; Powell, A. K.; Sessoli, R. *Phys. Rev. Lett.* **2008**, *100*, 247205-1.
 (15) Osa, S.; Kido, T.; Matsumoto, N.; Re, N.; Pochaba, A.; Mrozinski, J. *J. Am. Chem. Soc.* **2004**, *126*, 420.
 (16) Ferbinteanu, M.; Kajiwara, T.; Choi, K.-Y.; Nojiri, H.; Nakamoto, A.; Kojima, N.; Cimpoesu, F.; Fujimura, Y.; Takaishi, S.; Yamashita, M. *J. Am. Chem. Soc.* **2006**, *128*, 9008.
 (17) Zaleski, C. M.; Depperman, E. C.; Kampf, J. W.; Kirk, M. L.; Pecoraro, V. L. *Angew. Chem., Int. Ed.* **2004**, *43*, 3912.
 (18) Mishra, A.; Wernsdorfer, W.; Abboud, K. A.; Christou, G. *J. Am. Chem. Soc.* **2004**, *126*, 15648.
 (19) Ishikawa, N.; Sugita, M.; Ishikawa, T.; Koshihara, S.; Kaizu, Y. *J. Am. Chem. Soc.* **2003**, *125*, 8694.
 (20) Ishikawa, N.; Sugita, M.; Ishikawa, T.; Koshihara, S.; Kaizu, Y. *J. Phys. Chem. B* **2004**, *108*, 11265.
 (21) Ishikawa, N.; Sugita, M.; Wernsdorfer, W. *J. Am. Chem. Soc.* **2005**, *127*, 3650.
 (22) Ishikawa, N.; Sugita, M.; Wernsdorfer, W. *Angew. Chem., Int. Ed.* **2005**, *44*, 2931.
 (23) AIDamen, M. A.; Clemente-Juan, J. M.; Coronado, E.; Martí-Gastaldo, C.; Gaita-Ariño, A. *J. Am. Chem. Soc.* **2008**, *130*, 8874.
 (24) AIDamen, M. A.; Cardona-Serra, S.; Clemente-Juan, J. M.; Coronado, E.; Gaita-Ariño, A.; Martí-Gastaldo, C.; Luis, F.; Montero, O. *Inorg. Chem.* **2009**, *48*, 3467.
 (25) Rinehart, J. D.; Long, J. R. *J. Am. Chem. Soc.* **2009**, *131*, 12558.
 (26) Freedman, D. E.; Harman, W. H.; Harris, T. D.; Long, G. J.; Chang, C. J.; Long, J. R. *J. Am. Chem. Soc.* **2010**, *132*, 1224.
 (27) Harman, W. H.; Chang, C. J. *J. Am. Chem. Soc.* **2007**, *129*, 15128.

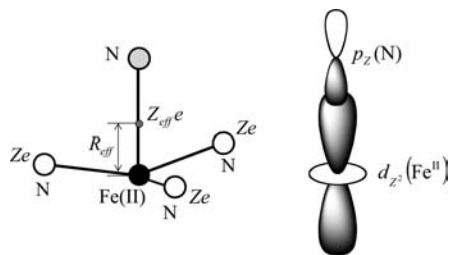


Figure 2. Illustration of the model.

We adopt the ligand field model, in which the three N-ligands 1, 2, and 3 are represented by their point charges ($Z = 1$), meanwhile the ligand 4 is represented by the effective charge Z_{eff} that is shifted from the ligand 4 toward the Fe(II) ion, with the distance between the effective charge and the iron ion being denoted as R_{eff} . This effective charge is introduced to take into account the above-mentioned strong covalence effect for the Fe(II)–N(4) bond. Such treatment of the covalence effects is somewhat similar to that proposed by Morrison and called the effective charge model (see refs 28,29 for the details). The model is illustrated by Figure 2. Then the LF Hamiltonian for the trigonal complex under consideration can be presented as follows:

$$H_{LF}({}^5D) = a_2 \langle r^2 \rangle B_2^0 Y_{20}({}^5D) + a_4 \langle r^4 \rangle B_4^0 Y_{40}({}^5D) + a_4 \langle r^4 \rangle \sqrt{2} [B_4^3 Y_{43}({}^5D) + B_4^{-3} Y_{4-3}({}^5D)] \quad (1)$$

where the parameters are given by

$$B_p^m = \frac{4\pi}{2p+1} (-1)^m \left[\frac{Z_{\text{eff}} e^2 Y_{p-m}(\theta_4, \varphi_4)}{R_{\text{eff}}^{p+1}} + \sum_{i=1}^3 \frac{Z e^2 Y_{p-m}(\theta_i, \varphi_i)}{R_i^{p+1}} \right] \quad (2)$$

$Z = 1$

The operators $Y_{pm}({}^5D)$ in eq 1 represent the spherical harmonics equivalents ($Y_{pm}({}^5D) = [2p+1]/(4\pi)^{1/2} \bar{O}_{pm}$, where \bar{O}_{pm} are the Racah operators) for the given 5D -term, which are closely related to the operator equivalents defined by Stevens³⁰ (see ref 31 for the details). It should be noted, however, that as distinguished from the Stevens operators, the operators $Y_{pm}({}^5D)$ as well as the Racah operators represent the irreducible tensors. This fact makes them preferable for computer calculations. Finally, in eq 1 a_2 and a_4 are the Stevens factors. For the ground 5D state of the Fe(II) ion these factors are the following:³²

$$a_2 \equiv \langle L \parallel \alpha \parallel L \rangle = -\frac{2}{21}, \quad a_4 \equiv \langle L \parallel \beta \parallel L \rangle = \frac{2}{63} \quad (3)$$

In calculations for the radial averages we use the values $\langle r^2 \rangle = 1.393$ au, $\langle r^4 \rangle = 4.496$ au.³²

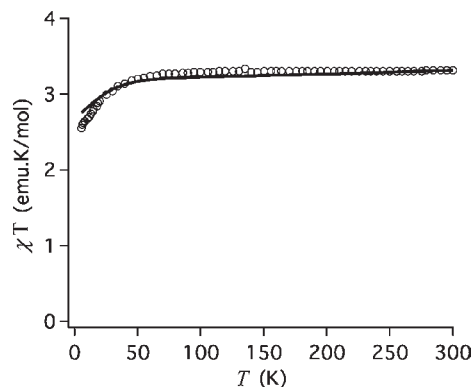


Figure 3. χT versus T curves for (open circles) experimental data obtained under applied dc field of 0.1 T,²⁶ (solid line) curve calculated with the best-fit parameters $Z_{\text{eff}} = 0.46$ and $R_{\text{eff}} = 0.78$ Å.

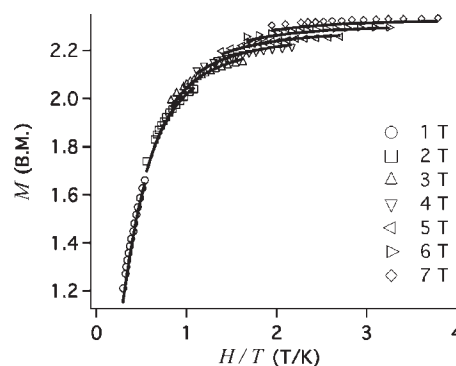


Figure 4. Low-temperature magnetization data for the $[(\text{tpaMes})\text{Fe}]^-$ complex for various applied dc fields: Experimental data²⁶ are shown by the symbols explained in the figure; curves calculated with the best-fit parameters $Z_{\text{eff}} = 0.46$ and $R_{\text{eff}} = 0.78$ Å are shown by solid lines.

The total Hamiltonian of the complex in the presence of the external magnetic field includes along with the LF potential also the spin–orbit coupling acting within the 5D term and Zeeman interaction, so one can write

$$H = H_{LF}({}^5D) + \lambda \mathbf{L} \cdot \mathbf{S} + \beta (\mathbf{L} + 2\mathbf{S}) \cdot \mathbf{H} \quad (4)$$

where λ is the SO parameter, \mathbf{H} is the applied magnetic field, \mathbf{L} and \mathbf{S} are the orbital angular momentum and spin operators, and β is the Bohr magneton. The value of the SO parameter λ will be fixed equal to -114 cm⁻¹.³²

Results and Discussion

The experimental magnetic data obtained in ref 26 (temperature dependence of the magnetic susceptibility in the form χT versus T , and low temperature magnetization under various applied dc fields) are shown in Figures 3, 4. Both the low-temperature slope of χT versus T curve (Figure 3) and a considerable separation between the isofield magnetization curves (Figure 4) indicate the presence of strong magnetic anisotropy. In ref 26 these magnetic data were fitted using the conventional spin-Hamiltonian

$$H = D \left[S_z^2 - \frac{1}{3} S(S+1) \right] + E(S_x^2 - S_y^2) + g\beta \mathbf{s} \cdot \mathbf{H} \quad (5)$$

where D and E are the axial and transverse ZFS parameters, respectively. In this way the authors obtained the following

(28) Morrison, C. A. *Lectures on Crystal Field Theory*, HDL-SR-82-2, Harry Diamond Laboratories Report, **1982**.

(29) Porcher, P.; Dos Santos, M. C.; Malta, O. *Phys. Chem. Chem. Phys.* **1999**, *1*, 397.

(30) Stevens, K. W. H. *Proc. Phys. Soc. A* **1952**, *65*, 209.

(31) Lindgård, P.-A.; Danielsen, O. *J. Phys. C: Solid State Phys.* **1974**, *7*, 1523.

(32) Abragam, A.; Bleaney, B. *Electron Paramagnetic Resonance of Transition Ions*; Clarendon: Oxford, England, 1970.

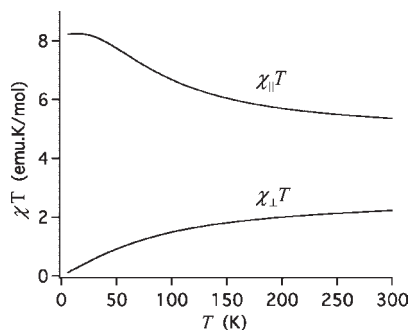


Figure 5. Principal values of the magnetic susceptibility tensor calculated with $Z_{\text{eff}} = 0.46$ and $R_{\text{eff}} = 0.78 \text{ \AA}$.

set of parameters: $D = -39.6 \text{ cm}^{-1}$, $E = -0.4 \text{ cm}^{-1}$, $g = 2.21$. The question to be answered in connection with this spin-Hamiltonian approach is whether it is valid for the Fe(II) complex under consideration. Note that the trigonal crystal field splits the atomic 5D term into the two orbital doublets (states with orbital angular momenta) and the orbital singlet. So to answer the question about the applicability of the spin-Hamiltonian, eq 5, one needs to know which state (orbital singlet or orbital doublet) proves to be the ground state one. The answer can be obtained in the framework of the model developed in Section 2.

It follows from the description presented in Section 2 that only two parameters remain unknown, namely, the value of the effective charge Z_{eff} and the distance R_{eff} . These two parameters are allowed to vary in the course of fitting the experimental χT versus T and M versus H , T curves. The best fit has been achieved for the values $Z_{\text{eff}} = 0.46$ and $R_{\text{eff}} = 0.78 \text{ \AA}$ with an agreement criterion value being equal to 3.34×10^{-4} . Note that both magnetization and magnetic susceptibility measurements have been included in this fit. One can see that the theoretical curves calculated with this set of parameters (Figures 3, 4, solid lines) are in a perfect agreement with the experimental data except the low temperature region for which the calculated χT curve is slightly above the experimental one. This deviation can be associated with the fact that our crystal field analysis is based on the consideration of the idealized C_{3v} symmetry thus neglecting the transverse anisotropy terms. The principal values of the magnetic susceptibility tensor calculated with the best-fit parameters (Figure 5) show that $\chi_{\parallel} T$ is significantly larger than $\chi_{\perp} T$ and hence we deal with the “negative” magnetic anisotropy, with the Z axis being the easy axis of the magnetization. This result is compatible with the slow relaxation of the magnetization observed for this system.

Now we are in the position to answer the question concerning the applicability of the spin-Hamiltonian approach to the analysis of the magnetic behavior of $[(\text{tpaMes})\text{Fe}]^{\text{II}}$ complex. Figure 6a (left side) shows that the ground LF term determined with the best-fit parameters is the orbital doublet. The expectation values of L_z calculated (with the set of the best-fit parameters) for the ground ligand-field term is $L_z = \pm 0.579$ indicating that the orbital angular momentum is not quenched in the case under consideration. This state undergoes the SO-splitting into the 6 sublevels as shown in the right side of Figure 6a (four doublets and two singlets, with the singlets being the highest excited levels). Such splitting can by no means be described by the ZFS spin-Hamiltonian $D[S_z^2 - 1/3S(S+1)]$ whose energy pattern for $S = 2$ includes three levels (two doublets and a singlet). Therefore we arrive at the conclusion

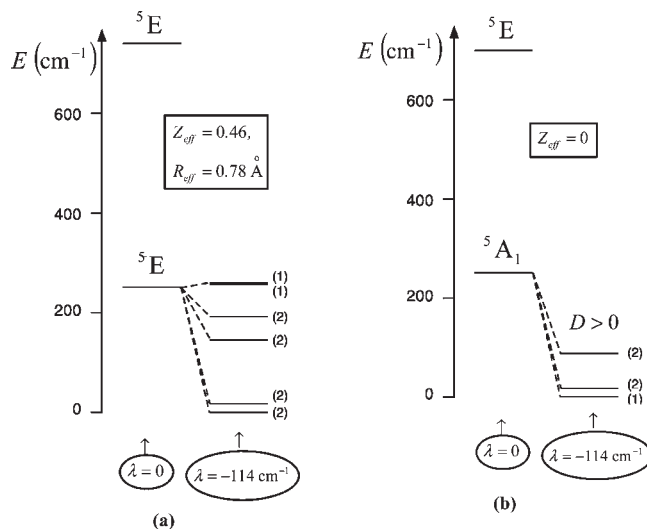


Figure 6. Low-lying parts of the energy pattern produced by the ligand field and the spin-orbital splitting of the ground terms: (a) calculation performed with the best-fit parameters; (b) sample calculation in the framework of the point charge model that neglects the covalence. In both cases the strongly excited upper level (5A_1 in case a and 5E in case b) are not shown. The multiplicities of the spin-orbital components are indicated in the parentheses, for example in the case of the term 5E (the multiplicity is 10) is split in 4 non-Kramers doublets and 2 singlets so that the total multiplicity is $4 \times 2 + 2 \times 1 = 10$.

that the spin-Hamiltonian formalism is irrelevant in the actual case, and the developed more general approach based on the Hamiltonian in eq 4 is unavoidable if one aims to adequately explain the magnetic behavior of the complex.

Figure 6 also demonstrates the crucial role of the covalency effects in the magnetic properties of the $[(\text{tpaMes})\text{Fe}]^{\text{II}}$ complex. In fact, comparing the energy pattern calculated with the best-fit parameters (Figure 6a) with that obtained in the framework of the point-charge model neglecting the covalence effects (Figure 6b) one can see that the inclusion of these effects changes the orbital multiplicity of the ground state. Indeed for $Z_{\text{eff}} = 0$ the ground state proves to be an orbital singlet (left side of Figure 6b). In this case the SO-mixing of the ground singlet with the excited orbital doublets splits the 5A_1 state into one singlet and two doublets (see the right side of Figure 6b). As distinguished from the case of the ground orbital doublet the splitting of the 5A_1 term can be described by the ZFS spin-Hamiltonian but the ZFS parameter D in this case is positive (the ground sublevel is a singlet), and hence this case is incompatible with the existence of the spin-reversal barrier and the observed slow relaxation of the magnetization. The strong covalence effect leads to the destabilization of the orbital singlet with respect to the orbital doublets and restores the relevant case shown in Figure 6a.

Conclusion

In this article we have successfully modeled the magnetic properties of the trigonal pyramidal complex $[(\text{tpaMes})\text{Fe}]^{\text{II}}$ which is the first mononuclear transition-metal complex behaving as a SMM. The proposed approach takes into account the trigonal LF splitting of the atomic 5D -term and the SO coupling. For the calculation of the LF parameters we adopted the model that takes into account both the point charges contribution and the covalence contribution, arising from the strong overlap between the d_{z^2} orbital of the Fe(II) ion and the p_z orbital of the apical nitrogen ligand. The covalence was modeled

by introducing the effective charge situated on the bond between the iron ion and the apical nitrogen ligand.

We have demonstrated that the ground LF term is the orbital doublet and the SO splitting of this term gives rise to the strong uniaxial magnetic anisotropy with the trigonal axis being the easy axis of the magnetization. These findings are in agreement with the existence of the magnetization reversal barrier and thus with the observed slow relaxation of magnetization. The obtained SO-splitting of the ground LF 5E -term cannot be described by the conventional ZFS spin-Hamiltonian and hence the spin-Hamiltonian approach used in ref 26 is inadequate in spite of the fact that it allowed to satisfactorily fit the magnetic data. Finally, the covalence was shown to play a crucial role in the magnetic behavior of the $[(\text{tpaMes})\text{Fe}]^-$ complex by destabilizing the orbital singlet and thus resulting in the highly anisotropic orbitally degenerate LF term 5E .

Summarizing one can say that the proposed approach might be helpful in the design and modeling of mononuclear

transition-metal magnets based on orbitally degenerate metal ions with controlled magnetic anisotropy and higher barrier for magnetization reversal. This approach is similar to the model reported by Fishman et al. to treat the Fe(II)Fe(III) bimetallic oxalates.³⁴ In some sense this approach can be regarded as a part of more general formalism suitable for the description of polynuclear orbitally degenerate systems in which the single-ion anisotropy is accompanied by the anisotropy arising from the orbitally dependent superexchange (see ref 33 for the details).

Acknowledgment. A.V.P., S.I.K., S.M.O., and O.S.R. gratefully acknowledge financial support from STCU (project N 5062). J.M.C.-J. and E.C. thank the Spanish MICINN (CSD2007-00010-consolider-ingenio in Molecular Nanoscience, MAT2007-61584, CTQ-2008-06720 and CTQ-2005-09385), Generalitat Valenciana (PROMETEO/2008/128), and the EU (MolSpinQIP project and ERC Advanced Grant SPINMOL) for financial support.

(33) Pali, A.; Tsukerblat, B.; Clemente-Juan, J. M.; Coronado, E. *Int. Rev. Phys. Chem.* **2010**, *29*, 135.

(34) Fishman, R. S.; Reboredo, F. A. *Phys. Rev. Lett.* **2007**, *99*, 217203. Fishman, R. S.; Clemente-León, M.; Coronado, E. *Inorg. Chem.* **2009**, *48*, 3039.